

## Mesopelagic carbon remineralization during the European Iron Fertilization Experiment

S. H. M. Jacquet,<sup>1,5</sup> N. Savoye,<sup>1,2</sup> F. Dehairs,<sup>1</sup> V. H. Strass,<sup>3</sup> and D. Cardinal<sup>4</sup>

Received 16 November 2006; revised 6 September 2007; accepted 4 October 2007; published 1 March 2008.

[1] The impact of iron fertilization on mesopelagic carbon (C) remineralization was assessed during the European Iron Fertilization Experiment (EIFEX) in the Southern Ocean by following the temporal change of excess particulate barium (also called biogenic or Ba<sub>xs</sub>) in the mesopelagic waters of a mesoscale eddy. Before the iron infusion the site was already sustaining a significant vertical flux of particles leading to organic remineralization in the mesopelagic. Approximately 35 d after the fertilization, mesopelagic Ba<sub>xs</sub> contents provided evidence of changes in surface particulate export and of enhanced and particularly fast remineralization extending down to 1000 m. At the end of the experiment (day 36) both export and remineralization decreased. Organic carbon remineralization took place mainly in the lower part of the mesopelagic zone (500–1000 m) and increased more than 5-fold during EIFEX, reaching values up to  $92 \pm 15 \text{ mg C m}^{-2} \text{ d}^{-1}$ . However, such remineralization rates are not particularly high when compared to other values reported for the natural Southern Ocean during summer. Though export and remineralization reached peak values around day 34, remineralization integrated over the 150 to 1000 m layer accounted only for  $13 \pm 1.4\%$  of the export at 150 m, suggesting that a substantial amount of exported carbon reached deeper in the water column. Compared to natural blooms in high-nutrient low-chlorophyll (HNLC) waters of the Southern Ocean, the Fe-induced bloom during EIFEX resulted in a lower ratio of remineralized organic carbon over exported carbon, similar to what we recently observed for natural Fe-replete conditions prevailing above the Kerguelen Plateau. Unexpected similarities and phase lags of profiles in the mesopelagic between casts sampled inside and outside the fertilized patch during EIFEX indicated that eddy dynamics were a determinant in setting particle patterns on a broad spatial scale exceeding the extent of the fertilization, thereby homogenizing the signals of mesopelagic remineralization.

**Citation:** Jacquet, S. H. M., N. Savoye, F. Dehairs, V. H. Strass, and D. Cardinal (2008), Mesopelagic carbon remineralization during the European Iron Fertilization Experiment, *Global Biogeochem. Cycles*, 22, GB1023, doi:10.1029/2006GB002902.

### 1. Introduction

[2] The Southern Ocean (S.O.) plays a key role in regulating the climate system and is recognized as an oceanic body particularly sensitive to climate change [Sarmiento *et al.*, 1998]. Model results indicate that it acts as a sink for atmospheric CO<sub>2</sub>, mainly because of phytoplankton uptake [Takahashi *et al.*, 2002]. Like other high-nutrient low-chlorophyll (HNLC) areas, primary production in the S.O. is mostly limited by the micronutrient iron, as demonstrated by

artificial mesoscale iron enrichment experiments (IronEx, SOIREE, EisenEX, SEEDS, SOFeX and SERIES cruises [Boyd *et al.*, 2000, 2004; Gervais *et al.*, 2002; Buesseler *et al.*, 2004, 2005; de Baar *et al.*, 2005]), confirming former phytoplankton incubation trials [Martin and Fitzwater, 1988; Hutchins and Bruland, 1998; Takeda, 1998]. All iron enrichment experiments showed an enhancement of primary production associated with a shift in the structure of the phytoplankton community toward larger diatoms [de Baar *et al.*, 2005]. However, because of the short duration of these experiments, the fate of the Fe-induced phytoplankton blooms was poorly recorded. Indeed, an increase in export production in the S. O. as a result of the iron addition was only reported for SOFeX [Buesseler *et al.*, 2005]. However, in assessing whether artificial iron fertilization in the S. O. could be a means of sequestering C deeper in the water column and mitigate the atmospheric CO<sub>2</sub> increase resulting from the anthropogenic activities [Martin, 1990], the magnitude of the export is not the only important parameter to infer this sequestration [Sarmiento *et al.*, 2004]. Indeed, the fate of the C exported under such iron

<sup>1</sup>Analytical and Environmental Chemistry Department, Vrije Universiteit Brussel, Brussels, Belgium.

<sup>2</sup>Now at Observatoire Aquitain des Sciences de l'Univers, UMR 5805 EPOC, CNRS, Université Bordeaux 1, Arcachon, France.

<sup>3</sup>Alfred Wegener Institute for Polar and Marine Research, Bremerhaven, Germany.

<sup>4</sup>Department of Geology, Royal Museum for Central Africa, Tervuren, Belgium.

<sup>5</sup>Now at CEREGE, UMR 6635, Europôle Méditerranéen de l'Arbois, Aix en Provence, France.

fertilization experiments is largely overlooked although remineralization in mesopelagic waters (150–1000 m) is responsible for the release of most of the C exported from the surface mixed layer (0–150 m) [Lampitt and Antia, 1997; Martin *et al.*, 1987; Sarmiento *et al.*, 1993; Suess, 1980]. Assessing mesopelagic C remineralization is pivotal to evaluate remineralization length scale and extent of the C export and sequestration in the deep ocean, and thus to simulations of the ocean's role in the global C cycle [Longhurst, 1995; Boyd *et al.*, 1999; François *et al.*, 2002; Passow and De la Rocha, 2006; Buesseler *et al.*, 2007; Biddanda and Benner, 1997].

[3] The present work aims to understand the impact of an artificial iron-induced bloom in terms of mesopelagic remineralization processes. Carbon remineralization was assessed from excess particulate barium ( $Ba_{xs}$ ) contents in the mesopelagic water column. Excess particulate Ba (mainly composed of barite microcrystal,  $BaSO_4$  [Dehairs *et al.*, 1980; Stroobants *et al.*, 1991]) within the mesopelagic zone increases over the growth season as a result of the export of biogenic aggregates from the mixed layer and their degradation at depth [Dehairs *et al.*, 1980, 1992, 1997]. The association of barite formation with bacterial degradation of organic matter, followed by the release of discrete barite microcrystals in the ambient water, led to the use of discrete barite crystals as a proxy for mesopelagic remineralization of exported biogenic material [Dehairs *et al.*, 1997, 2008; Cardinal *et al.*, 2005; Jacquet *et al.*, 2008]. An algorithm relating mesopelagic  $Ba_{xs}$  (meso- $Ba_{xs}$ ) contents to oxygen consumption [Shopova *et al.*, 1995; Dehairs *et al.*, 1997] allowed remineralized particulate organic carbon fluxes to be estimated for the mesopelagic layer.

[4] Here, we examine changes in mesopelagic carbon remineralization (150–1000 m) in response to the addition of iron during the European Iron Fertilization Experiment (EIFEX) [Smetacek, 2005], carried out in the Atlantic sector of the S.O. We expand on these results with a detailed analysis of the temporal evolution of mesopelagic  $Ba_{xs}$  in the context of a broader study of the biogeochemistry of the fertilized area, and in terms of its significance as a proxy for quantifying carbon remineralization. The present work is part of a multipronged approach which aims to determine the fate of an iron-induced bloom and associated sinking particles. The specific goal is to answer the question whether or not C export and sequestration increase significantly as a result of iron fertilization in the ocean.

## 2. Experiment and Methods

### 2.1. European Iron Fertilization Experiment

[5] The EIFEX cruise (ANT XXI/3 of R/V *Polarstern*; 21 January to 25 March 2004) was carried out in a mesoscale cyclonic eddy located in a meander of the polar front. The physical setting of the experiment is described by Strass *et al.* [2005]. The water mass in the eddy, centered at roughly 50°S–2°E, was characteristic of the Antarctic Circumpolar Current (low-temperature, HNLC conditions) and showed iron depletion (0.08–0.2 nM [Hoffmann *et al.*, 2006]). Seven tons of iron sulfate were added to an area of 150 km<sup>2</sup> on 12–13 February after an initial sampling to determine the

prefertilization conditions;  $T = -1$  reflects the conditions before the iron release, which occurred on day zero ( $T_0$ ). A second iron release into the previously fertilized patch was undertaken on 26–27 February (day 13). The outcome of the fertilizations was monitored over 35 d after the initial iron release. Samples were collected at stations both inside and outside the iron-fertilized patch (hereafter referred to as IN and OUT stations, respectively), though all stations reported in this study were located inside the eddy. IN and OUT patch stations were defined by surface parameters, e.g., photosynthetic efficiency index  $F_v/F_m$  (phytoplankton of iron-limited waters respond rapidly to iron addition by increasing their photosynthetic efficiency index), Fe, Chl *a* and  $pCO_2$  data, enabling the fertilized water to be easily followed.

[6] During EIFEX, Chl *a* concentrations increased more than fivefold by day 25 and then decreased toward the end of the experiment, while particulate organic matter followed a similar pattern, declining after day 29. These findings indicate the demise of the iron-induced bloom [Hoffmann *et al.*, 2006]. The massive increase in Chl *a* concentrations was mainly due to the growth of long chain-forming (*Chaetoceros* spp., *Fragilariopsis kerguelensis*, *Pseudo-nitzschia* spp.) and large single celled diatoms (*Thalassiothrix antarctica*, *Corethron inerme*, *Proboscia* spp., *Rhizosolenia* spp.) (data from P. Assmy *et al.*, personal communication, 2005). A deep and fast export has been clearly characterized during EIFEX, as revealed by <sup>234</sup>Th flux, profiling transmissometer and surface sediment data, microscopy observations and phytoplankton pigment analysis (N. Savoye and V. Strass, personal communication, 2005; O. Sachs *et al.*, personal communication, 2005).

### 2.2. Sampling and Analyses

[7] Sampling of suspended matter for particulate Ba measurements was performed at  $T = -1$ , 1 d prior to the first iron infusion and subsequently at the IN stations (on days 10, 21, 28, and 36) and the OUT stations (on days 11, 26 and 34). For each sampling event, seawater was sampled using Niskin bottles, usually at 16 depths between surface and 1000 m. Four to seven liters were filtered onto polycarbonate membranes 47 or 90 mm in diameter and having a porosity of 0.4  $\mu$ m. Samples were subsequently rinsed with Milli-Q grade water (<5 mL) to remove sea salt, dried (50°C) and stored in petri dishes for later analysis in the home-based laboratory. At that point, samples were digested using an HF/HCl/HNO<sub>3</sub> acid mixture and analyzed for Ba and other major and trace elements by ICP-AES (inductively coupled plasma–atomic emission spectrometry; Thermo Optek Iris Advantage) and ICP-QMS (inductively coupled plasma–quadrupole mass spectrometry; VG Plasma Quad 2+ Thermo Elemental) [Cardinal *et al.*, 2001]. In order to calculate biogenic barium (hereafter called excess Ba or  $Ba_{xs}$ ), total particulate Ba was corrected for lithogenic Ba using Al as the lithogenic reference element; we applied a mean value of 0.00112 (rsd = 16%) for the Ba/Al molar ratio as reported in the literature (see Reitz *et al.* [2004] (marine sediments) and Taylor and McLennan [1985] (crustal ratio)). Particulate Al contents during EIFEX range between 1 and 64 nM. Standard errors of ICP analyses are on average of 5% for total particulate Ba and

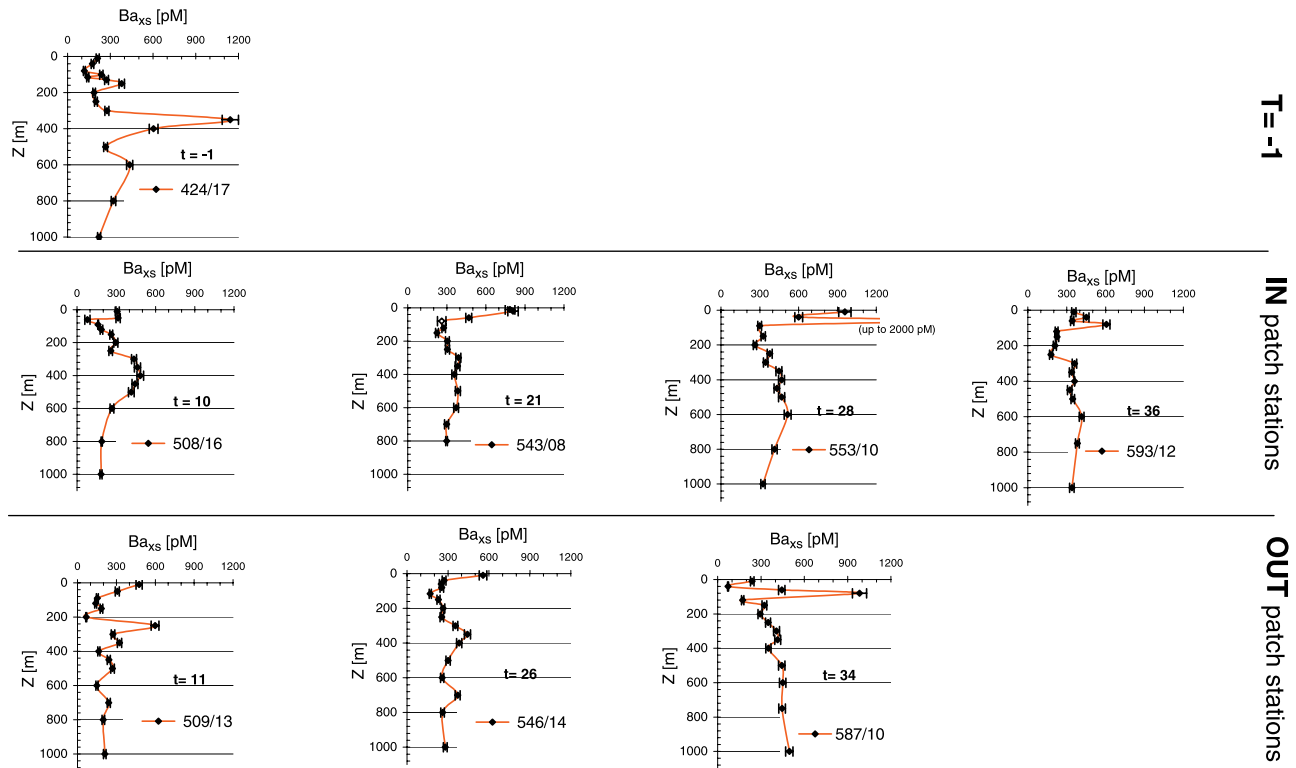


**Figure 1.** Particulate biogenic  $Ba_{xs}$  profiles (pM; 0–1000 m) at  $T = -1$ , IN-patch, and OUT-patch stations during the European Iron Fertilization Experiment (EIFEX).

14% for Al. Particulate excess Ba represented >96% of total particulate Ba at all stations. The standard uncertainty on  $Ba_{xs}$  data ranges from 5 to 6% [Ellison *et al.*, 2000] (see Figures 1 and 2). Moreover, analysis of filtered suspended matter using Scanning electron microscope coupled with energy dispersive X-ray detection revealed that barite ( $BaSO_4$ ) crystals accounted for nearly all of the mesopelagic  $Ba_{xs}$  contents during EIFEX. However, in the upper 150 m the situation is different. Here barite crystals were scarce while acantharians were observed to be major carriers of  $Ba_{xs}$  [Jacquet *et al.*, 2007].

### 2.3. C Remineralization

[8] As outlined above, the mesopelagic (meso-)  $Ba_{xs}$  signal which is mainly composed of barite microcrystals ( $BaSO_4$ ) [Dehairs *et al.*, 1980] builds up during the growth season [Dehairs *et al.*, 1997; Cardinal *et al.*, 2001, 2005] as the result of degradation and remineralization of particulate biogenic organic materials exported from the surface. Observations support that in a world ocean mostly undersaturated with barite [Monnin *et al.*, 1999; Rushdi *et al.*, 2000; Monnin and Cividini, 2006], these biogenic aggregates provide the necessary thermodynamic conditions for barite precipitation during organic matter remineralization, through sulphate and/or barium enrichment [Dehairs *et al.*, 1980, 2000; Bishop, 1988; Stroobants *et al.*, 1991]. The  $Ba_{xs}$ -barite water column distribution reflects production of

particulate Ba to take place below the upper mixed layer and to be ongoing into the twilight zone and even deeper, as recently emphasized by van Beek *et al.* [2007].

[9] The remineralized carbon in the mesopelagic layer was estimated using an algorithm relating mesopelagic  $Ba_{xs}$  contents to the rate of oxygen consumption as deduced from a 1-D advection-diffusion-consumption model applied on highly resolved and precise dissolved  $O_2$  profiles (2m binned data from CTD profiles) along 6°W in the Southern Ocean [Shopova *et al.*, 1995; Dehairs *et al.*, 1997]:

$$J_{O_2} = (\text{meso}Ba_{xs} - Ba_{\text{residual}})/17,200 \quad (1)$$

$$C_{\text{respired}} = Z \times J_{O_2} \times RR \quad (2)$$

where  $J_{O_2}$  is the  $O_2$  consumption ( $\mu\text{mol L}^{-1} \text{d}^{-1}$ ),  $C_{\text{respired}}$  is the amount of carbon mineralized (in  $\text{mmol C m}^{-2} \text{d}^{-1}$ ; further expressed in  $\text{mg C m}^{-2} \text{d}^{-1}$ ),  $Z$  is the thickness of the water column layer over which mesopelagic  $Ba_{xs}$  is calculated,  $RR$  is the respiration  $O_2$ :C molar ratio (we used a mean value of  $0.733 \pm 0.018$  for  $O_2$ :C ratios reported in literature [Broecker and Peng, 1982; Anderson and Winckler, 2005]),  $\text{meso-}Ba_{xs}$  is the  $Ba_{xs}$  amount that accumulates over the growth season and  $Ba_{\text{residual}}$  is the background  $Ba_{xs}$  signal at zero oxygen consumption, i.e., at zero organic C demand. The residual  $Ba_{xs}$  likely depends on the saturation state of the water with respect to

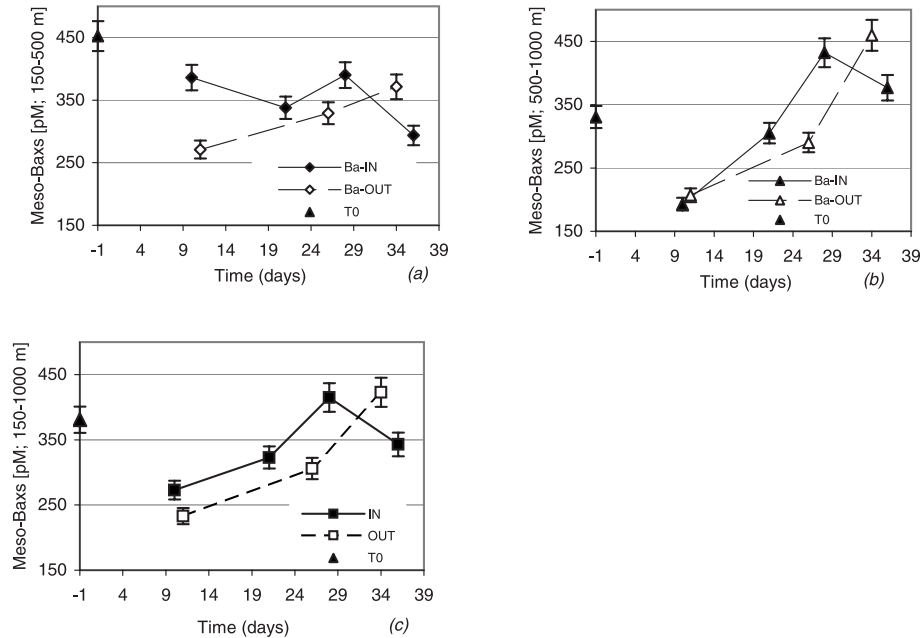


**Figure 2.** Depth-weighted average values of mesopelagic  $Ba_{xs}$  (pM) over a 37-d observation period during EIFEX; integration between (a) 150–500 m, (b) 500–1000 m, and (c) 150–1000 m.

barite. For the S.O. south of the PF, shown by *Monnin et al.* [1999] and *Monnin and Cividini* [2006] to be saturated for  $BaSO_4$  from surface to 2500 m, this residual  $Ba_{xs}$  is close to 180 pM [*Dehairs et al.*, 1997]. A residual  $Ba_{xs}$  value of 180 pM is close to the average  $Ba_{xs}$  contents observed at greater depth around 1000 m (i.e., below the mesopelagic  $Ba_{xs}$  maximum) in various sectors of the Southern Ocean [*Cardinal et al.*, 2001, 2005; *Jacquet et al.*, 2005] where input of  $Ba_{xs}$  as a result of export and remineralization is probably minimal, but where  $BaSO_4$  saturation still prevails [*Monnin et al.*, 1999; *Monnin and Cividini*, 2006]. We therefore considered a  $Ba_{xs}$  value of 180 pM zone as representative of the  $Ba_{xs}$  background in the mesopelagic zone, in accordance with *Dehairs et al.* [1997]. Proper assessment of the residual  $Ba_{xs}$  signal, however, would require winter data which at present are

not available. For assessment of POC mesopelagic remineralization from  $Ba_{xs}$  contents we assumed that the relationship given in equation (2) and established for the Atlantic sector of the S.O. south of the polar front [*Dehairs et al.*, 1997] applies for the present study area also located in the polar front area. The relative standard uncertainties on the slope and intercept ( $Ba_{residual}$ ) in equation (1) are 18.3 and 16.2%, respectively [*Shopova et al.*, 1995; *Dehairs et al.*, 1997], yielding relative standard uncertainties on  $C_{respired}$  (equation (2)) from 9 to 17% [*Ellison et al.*, 2000] (see Table 1).

### 3. Results

#### 3.1. Particulate Biogenic $Ba_{xs}$ Profiles

[10] Particulate biogenic  $Ba_{xs}$  profiles (0–1000 m) were measured at IN and OUT patch stations over a 37-d

**Table 1.** Depth-Weighted Average Values of Mesopelagic  $Ba_{xs}$  and C Remineralization Fluxes at  $T = -1$ , IN-Patch (Days 10, 21, 28, and 36) and OUT-Patch (Days 11, 26, and 34) Stations During the European Iron Fertilization Experiment

Time, d	Meso- $Ba_{xs}$ , pM			C Remineralization, mg C/m <sup>2</sup> /d, 150–1000 m	Standard Uncertainty, %
	150–500 m	500–1000 m	150–1000 m		
–1	452	330	381	78	15
10	386	193	273	31	12
21	338	305	323	40	10
28	390	432	415	92	16
36	294	377	343	61	14
11	271	207	233	14	9
26	329	290	306	45	13
34	371	460	423	96	17

observation period (Figure 1). In the upper 150 m acantharians (celestite,  $\text{SrSO}_4$ ' secreting protozoans) containing Ba as a minor element could explain essentially all  $\text{Ba}_{\text{xs}}$  present [Jacquet *et al.*, 2007]. This situation with nonbarite phases accounting for most excess Ba in surface waters was also reported by Cardinal *et al.* [2005], with carriers other than acantharians contributing to the surface water  $\text{Ba}_{\text{xs}}$  signal. Here, we focus on the mesopelagic zone where most of the remineralization of exported C is thought to take place [Martin *et al.*, 1987; Sarmiento *et al.*, 1993; Buesseler *et al.*, 2007] and where the meso- $\text{Ba}_{\text{xs}}$  signal is mainly composed of barite [Dehairs *et al.*, 1980; Jacquet *et al.*, 2007].

[11] Before the first iron infusion ( $T = -1$ ), a clear meso- $\text{Ba}_{\text{xs}}$  maximum was present between 300 and 400 m (Figure 1). The presence of a  $\text{Ba}_{\text{xs}}$  maximum, usually in the 150–500 m depth layer was also noted during previous Southern Ocean cruises [Dehairs *et al.*, 1992, 1997; Cardinal *et al.*, 2001, 2005; Jacquet *et al.*, 2005], but the maximum value observed in the present study (reaching 1150 pM) is quite high compared to previous studies. Such a high mesopelagic  $\text{Ba}_{\text{xs}}$  content indicates significant remineralization of organic matter was ongoing at the onset of the experiment. Because there is a time delay of a few days/weeks between a C export event and the response of the mesopelagic  $\text{Ba}_{\text{xs}}$  signal [Cardinal *et al.*, 2005], this remineralization must be associated with a bloom that occurred before the start of the EIFEX experiment. This is consistent with several other independent parameters like export production (based on  $^{234}\text{Th}$  flux data; N. Savoye, personal communication, 2005) and  $\text{fCO}_2$  data (R. Bellerby, personal communication, 2005). After the first iron infusion, a decrease in the meso- $\text{Ba}_{\text{xs}}$  maximum was observed during the first 10 d at IN-patch stations. However,  $\text{Ba}_{\text{xs}}$  contents between 250 and 600 m were still as high as 485 pM. Deeper in the water column, concentrations of  $\text{Ba}_{\text{xs}}$  decreased to 180 pM at 1000 m. From day 10 to 36 (at IN-patch stations), the meso- $\text{Ba}_{\text{xs}}$  maximum at 400 m tended to dissipate and  $\text{Ba}_{\text{xs}}$  increased in the deeper mesopelagic domain (up to 1000 m). This was a striking and rather unusual feature for S.O.  $\text{Ba}_{\text{xs}}$  profiles. By the end of the 37-d observation period, meso- $\text{Ba}_{\text{xs}}$  at IN-patch stations was rather homogeneous between 300 and 1000 m. A similar trend of increasing  $\text{Ba}_{\text{xs}}$  contents in the deeper mesopelagic zone was also observed at OUT-patch stations.

### 3.2. Depth-Weighted Average Values of $\text{Ba}_{\text{xs}}$

[12] As mentioned above,  $\text{Ba}_{\text{xs}}$  contents between 150 and 500 m decreased with time, while they appeared to increase between 500 and 1000 m. We will now consider temporal mesopelagic  $\text{Ba}_{\text{xs}}$  changes over both these depth layers in more detail. Depth-weighted average values (i.e.,  $\text{Ba}_{\text{xs}}$  inventories divided by the height of the considered water column section) integrated over 150–500 m ( $\text{Ba}_{500}$ ) and 500–1000 m ( $\text{Ba}_{1000}$ ) are shown in Figure 2 and Table 1 for both IN and OUT stations.  $\text{Ba}_{500}$  was high at the start of the experiment ( $T = -1$ ) and decreased within the first 11 d (OUT) and 21 d (IN), reflecting the dissipation of the initial mesopelagic  $\text{Ba}_{\text{xs}}$  maximum (Figure 2a). Then, depth weighted average values increased slightly with time and decreased again by the very end of the experiment. Note that  $\text{Ba}_{500}$  obtained at day 28 at IN-patch stations (390 pM)

was lower in magnitude than those naturally occurring before the iron infusion (452 pM;  $T = -1$ ). In contrast, the  $\text{Ba}_{1000}$  decrease stopped at day 10 (IN) and day 11 (OUT) and then, notably, increased until days 28 and 34 for IN and OUT stations, respectively. After reaching a maximum of 432 and 460 pM at IN and OUT stations, respectively,  $\text{Ba}_{1000}$  finally decreased once again until day 36 at IN-patch stations (Figure 2b).  $\text{Ba}_{500}$  and  $\text{Ba}_{1000}$  maximum values during EIFEX (at  $T = -1$ , as well as at days 28 for IN stations and 34 for OUT stations) were relatively small in comparison to other values reported for S.O. summer conditions (i.e., 500 to 600 pM [Dehairs *et al.*, 1992, 1997; Cardinal *et al.*, 2001, 2005; Jacquet *et al.*, 2005]).

[13] Depth weighted average  $\text{Ba}_{\text{xs}}$  values between 150–1000 m at IN and OUT stations showed a similar progression of the  $\text{Ba}_{\text{xs}}$  signal throughout the experiment, though OUT stations lagged behind by 5 to 6 d (Figure 2c). Such similarities in  $\text{Ba}_{\text{xs}}$  stocks may have resulted from particle sedimentation patterns and eddy dynamics (see discussion below). Between days 10 and 21 (at IN-patch stations), meso- $\text{Ba}_{\text{xs}}$  increased slightly (Figure 2c), reflecting enhanced mesopelagic remineralization processes, while the export flux at 150 m remained high ( $^{234}\text{Th}$  flux data; N. Savoye, personal communication, 2005). From Figures 2a and 2b, it is obvious that  $\text{Ba}_{\text{xs}}$  inventories between 150–1000 m were mainly driven by  $\text{Ba}_{1000}$ . At IN-patch stations  $\text{Ba}_{500}$  decreases between  $T = -1$  and day 21 were similar to  $\text{Ba}_{1000}$  increases between days 10 and 21 (Table 1). It is thus possible that remineralization fueled by the preinfusion bloom was continued until day 21. After days 21 (IN stations) and 26 (OUT stations), the depth-weighted average  $\text{Ba}_{\text{xs}}$  values showed a strong increase. At IN stations this feature coincided with a distinct dip at day 21 and a decline after day 25 of Chl *a* and particulate organic carbon, nitrogen, phosphorus and biogenic silica contents in surface waters (at 20 m) [Hoffmann *et al.*, 2006] and was associated with an increase in carbon export (based on  $^{234}\text{Th}$  flux data; N. Savoye, personal communication, 2005). In addition, the decline of the different biomass parameters in the mixed layer at the end of the experiment indicates that field observations extended sufficiently long to catch the bloom and witness its decay [Hoffmann *et al.*, 2006]. The coincidence of mesopelagic  $\text{Ba}_{\text{xs}}$  variations with variations in surface biomass and carbon export suggests that the iron fertilization induced (1) a close coupling between surface waters and the mesopelagic in terms of organic matter export and processing at depth and (2) the spreading-out of remineralization over a deeper water column (till depths of at least 1000 m).

[14] Depth weighted average  $\text{Ba}_{\text{xs}}$  values (150–1000 m) were translated into carbon remineralization rates using equations (1) and (2) given above. These rates ranged from 14 to 96  $\text{mgC m}^{-2} \text{d}^{-1}$  (Table 1).

## 4. Discussion

### 4.1. Fate of Exported Organic Material During EIFEX

[15] The pattern of remineralization described above can be explained by superposition of two events of particle

sedimentation: slow sedimentation from the natural pre-fertilization bloom and fast sedimentation from the bloom that was stimulated by artificial iron supply. The slow sedimentation is evident from the opposite temporal developments of IN patch  $Ba_{xs}$  stocks in the layers between 150–500 and 500–1000 m (Figure 2), as well as by the downward propagation of the pre-fertilization mesopelagic  $Ba_{xs}$  maximum seen in Figure 1, which also flattens and broadens during the 5 weeks of the experiment. The fast sedimentation event is suggested by the temporal  $Ba_{xs}$  stock increase, which occurs between days 21 and 34 in both layers 150–500 and 500–1000 m depth. Our results thus indicate that shortly after the first evidence of enhanced particle export from the mixed layer ( $^{234}\text{Th}$  flux data from N. Savoye, personal communication, 2005) the biogenic matter originating from the induced bloom had reached deep into the mesopelagic zone. Such findings are in accordance with profiling transmissometer data showing an increase in particulate organic C stocks between 150–500 m during the first 3 weeks and which extend down to 3000 m after day 24 (data from V. Strass et al., personal communication, 2005). However, the maximum C remineralization reached at day 28 (IN;  $92 \pm 15 \text{ mgC m}^{-2} \text{ d}^{-1}$ ; Table 1) is not particularly high when compared with other values reported for Southern Ocean summer conditions (up to  $140 \text{ mgC m}^{-2} \text{ d}^{-1}$  in the Indian sector [Jacquet et al., 2005]). Moreover, unexpected similarities in remineralization fluxes at mesopelagic depths between IN- and OUT-patch stations suggest that particle export at OUT-patch stations was also impacted by the fertilization. OUT-patch surface waters, in contrast, did not show any impact of fertilization, and were distinct by phytoplankton communities, particulate organic materials and Chl *a* values which remained more or less at the pre-fertilization level [Hoffmann et al., 2006]. The same holds for export production which stayed high but relatively constant in the mixed layer at OUT-patch stations and increased only slightly during the experiment ( $^{234}\text{Th}$  flux data from N. Savoye, personal communication, 2005). The possibility that mesopelagic waters sampled at OUT stations were influenced by the Fe-fertilized patch (i.e., by mixed layer waters with high POC concentration) can be the consequence of the eddy circulation, in which the speed of rotation changes with depth. In the simplest example where the speed decreases linearly with depth from highest values at the surface to zero at the sea floor, a patch in the mixed layer would drift over the slower moving layers below. Therefore deeper “OUT” layers should also receive particles from “IN” surface waters but with a longer time lag than “IN” deep layers. We remind that the label “IN” and “OUT-patch” stations was defined using surface parameters, which do not describe the conditions at mesopelagic depths. The vanishing differences between IN and OUT-patch casts in C remineralization and the unusual  $Ba_{xs}$  profiles (i.e., homogeneous mesopelagic  $Ba_{xs}$  signals at IN and OUT stations spreading down to 1000 m) would thus result from horizontal mixing in the deeper mesopelagic. This explanation fits with results from P. Assmy et al. (personal communication, 2005), indicating clear differences in diatom abundances between IN and OUT stations in the upper 350 m, while in the deeper water

column, down to 3500 m, abundances of diatoms frustules were similar (and high) at IN and OUT patch sites, emphasizing the impact of the eddy vertical shear on the distribution of particles. Overall, these findings suggest that mesopelagic carbon remineralization, both at IN and OUT stations, reflect the system’s response to iron addition during EIFEX.

[16] As outlined above, the present work is part of a multipronged approach whose target is the fate of an iron-induced bloom and associated sinking particles. In particular, our approach is based on the comparison between  $Ba_{xs}$ -based carbon remineralization and  $^{234}\text{Th}$ -based export production;  $^{234}\text{Th}$  data will be discussed in more detail in an upcoming paper. Briefly, N. Savoye (personal communication, 2005) observed that export production at 150 m was high at  $T = -1$  and that fluxes at both IN and OUT stations remained high and constant during the first 21 d (referred to as the first period) of the experiment. Day 21 is considered as the switch-over between the situation before and after the impact of the fertilization. N. Savoye (personal communication, 2005) also observed that export production at OUT stations increased slightly from day 17 to day 34, while at IN stations it decreased to reach lowest values at days 20–24. From day 24 to day 32 a huge increase of carbon export occurred coinciding with a massive sinking of large diatoms (P. Assmy et al., personal communication, 2005).

[17] To estimate remineralization efficiency in mesopelagic waters we calculated total C remineralization and total export production (Figure 3). Total C export production and total C remineralization are given by the weighted average of IN and OUT fluxes to the water column underlying the drifting fertilized patch. A drift of the patch in the mixed layer relative to the deeper layers results from the vertical shear in the circular flow of the eddy (see above paragraph 15). Relative to the sea floor, the trace of the drifting patch resembles a ring whose area is roughly four times the area of the fertilized patch (V. Strass et al., personal communication, 2005). Total C export and remineralization were calculated as follows:  $(X_{\text{IN}} + 3 X_{\text{OUT}})/4$  ( $X$  being either export or remineralization). The overlap in the timing of both processes emphasizes the intensity of carbon export and its close coupling to remineralization during EIFEX. At day 34, when maxima of total carbon export and remineralization were reached, total remineralization in the 150–1000 m depth layer accounts for  $13 \pm 1.4\%$  of the total carbon export at 150 m. This suggests that a large fraction of the export is transported below 1000 m. Moreover, from days 11–21 to days 21–34, remineralization of the carbon export at depth increased from 5 to  $20 \pm 2\%$ , indicating that the high export over remineralization ratio just after fertilization decreased over time.

[18] Comparison of C export and remineralization for EIFEX is however subject to caution, because of the mismatch of sampling times and a rather coarse sampling frequency. However our findings corroborate other observations during EIFEX, such as an increase of the particle load in the depth range 1000–3000 m evident from optical data (V. Strass et al., personal communication, 2005) as well as the presence of highly reactive biogenic particles in the

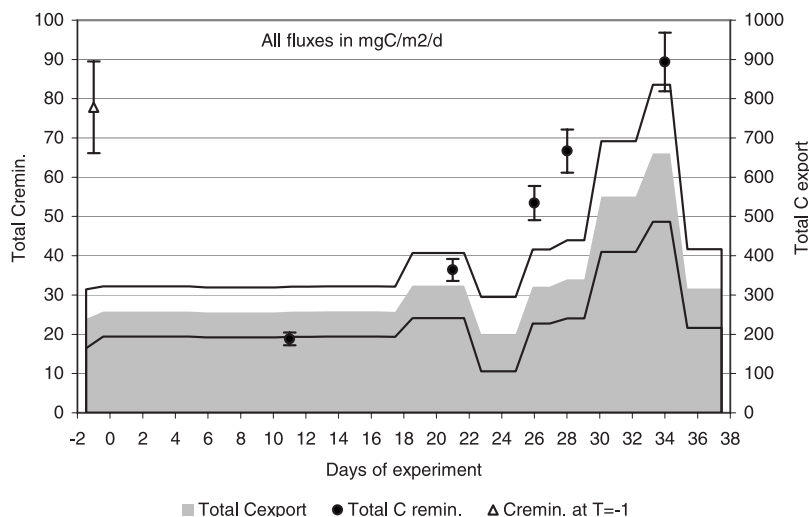


**Figure 3.** Total C remineralization (150–1000 m; dots) and total export (0–150 m) fluxes ( $\text{mg C m}^{-2} \text{d}^{-1}$ ; gray area) over a 37-d observation period during EIFEX. Continuous black lines represent standard uncertainties on total carbon export.

nepheloid layer and the surface sediments (O. Sachs et al., personal communication, 2005).

#### 4.2. Deeper Mesopelagic Remineralization Induced by Iron Fertilization?

[19] The finding that the effect of iron addition during EIFEX led to a fast and deep mesopelagic C remineralization has several important implications. It indicates that the iron fertilization not only enhanced particle flux within the fertilized surface water, it also significantly influenced the fate of these sinking particles once they left the upper layers. Our results suggest that organic carbon exported from the surface layer was rapidly subject to partial remineralization which reached at least down to 1000 m and potentially deeper (Figure 2). This implies also that the part of sinking particles were probably exported beyond 1000 m, as attested by the presence of fresh organic material in the nepheloid layer and the surface sediment (O. Sachs et al., personal communication, 2005).

[20] Our observations at  $T = -1$ , just prior to the fertilization, indicate that mesopelagic remineralization reached  $33 \pm 7.6\%$  of carbon export (the latter from <sup>234</sup>Th flux data). As compared to natural blooms, the Fe induced bloom during EIFEX yields a lower total remineralized carbon to total exported carbon ratio:  $13 \pm 1.4\%$  at day 34 and from 5 to  $20 \pm 2\%$  over the whole duration of the experiment. This remineralization efficiency is close to summer values reported by *Jacquet et al.* [2008] for the Kerguelen Plateau (9 to 13%) during the KEOPS cruise. Contrasting with this, the off-shelf remineralization efficiency during KEOPS ranged from 18 to 39% of the carbon export [*Jacquet et al.*, 2008], similar to what is observed during EIFEX before the Fe release ( $33 \pm 7.6\%$  at  $T = -1$ ). For the Kerguelen Plateau area, *Jacquet et al.* [2008] report that differences in trophic structure and in composition of the diatom community (larger cells above the plateau) could possibly explain the difference in remineralization rate as

well as in transfer efficiency between on-shelf and off-shelf mesopelagic waters. Other studies in the natural open S.O. environment also report larger % of exported organic carbon being remineralized, mainly in the upper mesopelagic, compared to observations during EIFEX. For instance, *Cardinal et al.* [2005] report remineralization at the PFZ in the Australian sector (WOCE SR3 transect) to reach 40% of new production during spring and close to 100% during summer.

[21] Overall, results suggest that export from large diatom-dominated blooms is less prone to remineralization, probably because of a faster transfer of matter through the water column leaving less time for mesopelagic remineralization to occur, though the effect of low temperature on lowering remineralization by heterotrophs cannot be excluded [see *Laws et al.*, 2000]. The shape of the  $Ba_{xs}$  profiles and the similarities between meso- $Ba_{xs}$  stocks at IN and OUT stations (both located within the eddy), suggest that they were influenced by eddy dynamics and could be taken to reflect convective transport of material from the surface layer to the ocean's interior, as reported for instance by *van Haren et al.* [2006] for a Mediterranean eddy. However, during EIFEX, the density structure of the eddy was monitored throughout the experiment and was always found to be stable, precluding convection. The eddy itself was observed to persist with rather unchanged rotational velocity beyond the end of the experiment, excluding the slumping of isopycnals as a possible mechanism for the vertical transport of matter. Rapid sinking of plankton aggregates which formed at the decline of the iron-induced bloom was the evident process during EIFEX. However, similarities and phase lags of profiles in the mesopelagic zone between IN and OUT patch stations indicate that export and remineralization did not solely reflect the direct impact of iron fertilization, and therefore upscaling EIFEX results to the whole Southern Ocean is risky. While eddy dynamics per se undoubtedly have an impact on plankton

blooming, export and fate of carbon on the contrary are clearly a matter mainly of biology, with grazing pressure, if significant, impeding high carbon export ratios [see Benitez-Nelson et al., 2007; Lam and Bishop, 2007]. On the contrary, when grazing pressure is low(er), heterotrophic bacteria will control mineralization of sinking plankton detritus [see McGillicuddy et al., 2007; Lam and Bishop, 2007; Jacquet et al., 2008]. Although the remineralization:export ratio during the EIFEX experiment is rather low and indicates deep C sequestration to occur, it should be stressed that the induced export event was short and the enhancement of export flux rather moderate.

[22] **Acknowledgments.** We thank the captain and crew of R.V. *Polarstern* for their assistance during work at sea. We are indebted to chief scientist Victor Smetacek (AWI, Germany) for his skillful leadership during the cruise and to Ingrid Vöge (AWI, Germany) for help during sampling and measurements on board. Jacques Navez and Laurence Monin (MRAC, Tervuren) greatly helped during sample processing and element analysis by ICP-AES and ICP-QMS. Philip Assmy and Oliver Sachs (AWI, Germany) are warmly thanked for having shared their data prior to publication. This research was supported by the Federal Belgian Science Policy Office under SPSP Programs on Global Change, Ecosystems and Biodiversity, Brussels, Belgium (BELCANTO network contracts EV/37/7C, EV/03/7A, SD/CA/03A), the Vrije Universiteit Brussel under grant GOA22, and the Research Foundation Flanders via contract G.0021.04.

## References

- Anderson, R. F., and G. Winckler (2005), Problems with paleoproductivity proxies, *Paleoceanography*, *20*, PA3012, doi:10.1029/2004PA001107.
- Benitez-Nelson, C. R., et al. (2007), Mesoscale eddies drive increased silica export in the subtropical Pacific Ocean, *Science*, *316*, 1017–1021.
- Biddanda, B., and R. Benner (1997), Major contribution from mesopelagic plankton to heterotrophic metabolism in the upper ocean, *Deep Sea Res., Part I*, *44*(12), 2069–2085.
- Bishop, J. K. B. (1988), The barite-opal-organic carbon association in oceanic particulate matter, *Nature*, *332*(6162), 341–343.
- Blain, S., et al. (2007), Effect of natural iron fertilization on carbon sequestration in the Southern Ocean, *Nature*, *446*, 1070–1074.
- Boyd, P. W., R. H. Goldblatt, and P. J. Harrison (1999), Mesozooplankton grazing manipulations during in vitro iron enrichment studies in the NE subarctic Pacific, *Deep Sea Res., Part II*, *46*(11–12), 2645–2668.
- Boyd, P. W., et al. (2000), Phytoplankton bloom upon mesoscale iron fertilization of polar Southern Ocean waters, *Nature*, *407*, 695–702.
- Boyd, P. W., et al. (2004), The decline and fate of an iron-induced subarctic phytoplankton bloom, *Nature*, *428*, 549–553.
- Broecker, W. S., and T. H. Peng (1982), *Tracer in the Sea*, 690 pp., Lamont-Doherty Geol. Obs., Columbia Univ., Eldigio Press, New York.
- Buesseler, K., J. E. Andrews, S. M. Pike, and M. A. Charette (2004), The effect of iron fertilization on carbon sequestration in the Southern Ocean, *Science*, *304*, 414–417.
- Buesseler, K., J. E. Andrews, S. M. Pike, M. A. Charette, L. E. Goldson, M. A. Brzezinski, and V. P. Lance (2005), Particle export during the Southern Ocean Iron Experiment (SoFex), *Limnol. Oceanogr.*, *50*, 311–327.
- Buesseler, K. O., et al. (2007), Revisiting carbon flux through the ocean's twilight zone, *Science*, *316*, 567–570.
- Cardinal, D., F. Dehairs, T. Cattaldo, and L. André (2001), Geochemistry of suspended particles in the subantarctic and polar frontal zones south of Australia: Constraints on export and advection processes, *J. Geophys. Res.*, *106*(C12), 31,637–31,656.
- Cardinal, D., N. Savoye, T. W. Trull, L. André, E. Kopczynska, and F. Dehairs (2005), Particulate Ba distributions and fluxes suggest latitudinal variations of carbon mineralization in the Southern Ocean, *Deep Sea Res., Part II*, *52*, 355–370.
- de Baar, H. J. W., et al. (2005), Synthesis of iron fertilization experiments: From the Iron Age in the Age of Enlightenment, *J. Geophys. Res.*, *110*, C09S16, doi:10.1029/2004JC002601.
- Dehairs, F., R. Chesselet, and J. Jedwab (1980), Discrete suspended particles of barite and the barium cycle in the open ocean, *Earth Planet. Sci. Lett.*, *49*, 528–550.
- Dehairs, F., W. Baeyens, and L. Goeyens (1992), Accumulation of suspended barite at mesopelagic depths and export production in the Southern Ocean, *Science*, *258*, 1332–1335.
- Dehairs, F., D. Shopova, S. Ober, C. Veth, and L. Goeyens (1997), Particulate barium stocks and oxygen consumption in the Southern Ocean mesopelagic water column during spring and early summer: Relationship with export production, *Deep Sea Res., Part II*, *44*(1–2), 497–516.
- Dehairs, F., N. Fagel, A. N. Antia, R. Peinert, M. Elskens, and L. Goeyens (2000), Export production in the Bay of Biscay as estimated from barium-barite in settling material: A comparison with new production, *Deep Sea Res., Part I*, *47*(4), 583–601.
- Dehairs, F., et al. (2008), Particulate Ba and mesopelagic C remineralization at stations ALOHA and K2 during VERTIGO 1 and 2, *Deep Sea Res., Part II*, in press.
- Ellison, S. L. R., M. Rosslein, and A. Williams (Eds.) (2000), *Eurachem/CITAC Guide CG4, Quantifying Uncertainty in Analytical Measurement*, 2nd edition, 120 pp., EURACHEM Secretariat, BAM, Berlin.
- Fielding, S., et al. (2001), Mesoscale subduction at the Almeria-Oran front. Part 2: Biophysical interaction, *J. Mar. Syst.*, *30*, 287–304.
- François, R., S. Honjo, R. Krishfield, and S. Manganini (2002), Factors controlling the flux of organic carbon to the bathypelagic zone of the ocean, *Global Biogeochem. Cycles*, *16*(4), 1087, doi:10.1029/2001GB001722.
- Gervais, F., U. Riebesell, and M. Y. Gorbunov (2002), Changes in primary productivity and chlorophyll a in response to iron fertilization in the southern polar frontal zone, *Limnol. Oceanogr.*, *47*, 1324–1335.
- Hoffmann, L. J., I. Peeken, K. Lochte, P. Assmy, and M. Veldhuis (2006), Different reactions of Southern Ocean phytoplankton size classes to iron fertilization, *Limnol. Oceanogr.*, *51*(3), 1217–1229.
- Hutchins, D. A., and K. W. Bruland (1998), Iron-limited diatom growth and Si:N uptake ratios in a coastal upwelling regime, *Nature*, *393*, 561–564.
- Jacquet, S. H. M., F. Dehairs, D. Cardinal, J. Navez, and B. Delille (2005), Barium distribution across the Southern Ocean frontal system in the Crozet-Kerguelen Basin, *Mar. Chem.*, *95*(3–4), 149–162.
- Jacquet, S. H. M., J. Henjes, F. Dehairs, A. Worobiec, N. Savoye, and D. Cardinal (2007), Particulate Ba-barite and acantharians in the Southern Ocean during the European Iron Fertilization Experiment (EIFEX), *J. Geophys. Res.*, *112*, G04006, doi:10.1029/2006JG000394.
- Jacquet, S. H. M., F. Dehairs, N. Savoye, I. Obernosterer, U. Christaki, C. Monnin, and D. Cardinal (2008), Mesopelagic organic carbon mineralization in the Kerguelen Plateau region tracked by biogenic particulate Ba, *Deep Sea Res., Part II*, in press.
- Lam, P. J., and J. K. B. Bishop (2007), High biomass, low export regimes in the Southern Ocean, *Deep Sea Res., Part II*, *54*(5–7), 601–638.
- Lampitt, R. S., and A. N. Antia (1997), Particle flux in deep seas: Regional characteristics and temporal variability, *Deep Sea Res., Part II*, *44*(8), 1377–1403.
- Laws, E. A., P. G. Falkowski, W. O. Smith, H. Ducklow, and J. J. McCarthy (2000), Temperature effects on export production in the open ocean, *Global Biogeochem. Cycles*, *14*(4), 1231–1246.
- Longhurst, A. (1995), Seasonal cycles of pelagic production and consumption, *Prog. Oceanogr.*, *36*(2), 77–167.
- Martin, J. H. (1990), Glacial to interglacial CO<sub>2</sub> change: The iron hypothesis, *Paleoceanography*, *5*, 1–13.
- Martin, J. H., and S. E. Fitzwater (1988), Iron deficiency limits phytoplankton growth in the north-east Pacific subarctic, *Nature*, *331*, 341–343.
- Martin, J. H., G. A. Knauer, D. M. Karl, and W. W. Broenkow (1987), VERTEX: Carbon cycling in the northeast Pacific, *Deep Sea Res., Part A*, *34*, 267–285.
- McGillicuddy, D. J., et al. (2007), Eddy/wind interactions stimulate extraordinary mid-ocean plankton blooms, *Science*, *316*, 1021–1026.
- Monnin, C., and D. Cividini (2006), The saturation state of the world's ocean with respect to (Ba, Sr) SO<sub>4</sub> solid solution, *Geochim. Cosmochim. Acta*, *70*, 3290–3298.
- Monnin, C., C. Jeandel, T. Cattaldo, and F. Dehairs (1999), The marine barite saturation state of the world's ocean, *Mar. Chem.*, *64*(3–4), 253–261.
- Passow, U., and C. L. De la Rocha (2006), Accumulation of mineral ballast on organic aggregates, *Global Biogeochem. Cycles*, *20*, GB1013, doi:10.1029/2005GB002579.
- Reitz, A., K. Pfeifer, G. J. de Lange, and J. Klump (2004), Biogenic barium and the detrital Ba/Al ratio: A comparison of their direct and indirect determination, *Mar. Geol.*, *204*, 289–300.
- Rushdi, A. I., J. McManus, and R. W. Collier (2000), Marine barite and celestite saturation in seawater, *Mar. Chem.*, *69*(1–2), 19–31.
- Sarmiento, J. L., R. D. Slater, M. J. R. Fasham, H. W. Ducklow, and J. R. Toggweiler (1993), A seasonal three-dimensional ecosystem model of nitrogen cycling in the North Atlantic photic zone, *Global Biogeochem. Cycles*, *7*(2), 417–450.
- Sarmiento, J. L., M. C. Hughes, R. J. Stouffer, and S. Manabe (1998), Simulated response of the ocean carbon cycle to anthropogenic climate warming, *Nature*, *393*, 245–249.

- Sarmiento, J. L., J. Dunne, and R. A. Armstrong (2004), Do we understand the ocean's biological pump?, *U. S. Joint Global Ocean Flux Study Newsl.*, 12(4), 1–5.
- Shopova, D., F. Dehairs, and W. Baeyens (1995), A simple model of biogeochemical element distribution in the oceanic water column, *J. Mar. Syst.*, 6, 331–344.
- Smetacek, V. (2005), Fahrabschnitt ANT XXI/3 Kapstadt–Kapstadt (21.01.04–25.03.04), 1. Introduction, *Rep. Polar Mar. Res.*, 500, 3–7.
- Strass, V., B. Cisewski, S. Gonzales, H. Leach, K.-D. Loquay, H. Prandke, H. Rohr, and M. Thomas (2005), The physical setting of the European Iron Fertilization Experiment 'EIFEX' in the Southern Ocean, *Rep. Polar Mar. Res.*, 500, 15–49.
- Stroobants, N., F. Dehairs, L. Goeyens, N. Vanderheijden, and R. Van Grieken (1991), Barite formation in the Southern Ocean water column, *Mar. Chem.*, 35, 411–421.
- Suess, E. (1980), Particulate organic carbon flux in the ocean-surface productivity and oxygen utilization, *Nature*, 288, 260–263.
- Takahashi, T., et al. (2002), Global sea-air CO<sub>2</sub> flux based on climatological surface ocean pCO<sub>2</sub>, and seasonal biological and temperature effects, *Deep Sea Res., Part II*, 49(9–10), 1601–1622.
- Takeda, S. (1998), Influence of iron availability on nutrient consumption ratio of diatoms in oceanic waters, *Nature*, 393, 774–777.
- Taylor, S. R., and S. M. McLennan (1985), *The Continental Crust: Its Composition and Evolution*, 312 pp., Blackwell Sci., Malden, Mass.
- van Beek, P., R. François, M. Conte, J. L. Reyss, M. Souhaut, and M. Charette (2007), Ra-228/Ra-226 and Ra-226/Ba ratios to track barite formation and transport in the water column, *Geochim. Cosmochim. Acta*, 71(1), 71–86.
- van Haren, H., C. Millot, and I. Taupier-Letage (2006), Fast deep sinking in Mediterranean eddies, *Geophys. Res. Lett.*, 33, L04606, doi:10.1029/2005GL025367.
- 
- D. Cardinal, Department of Geology, Royal Museum for Central Africa, Leuvensesteenweg 13, Tervuren B-3080, Belgium.
- F. Dehairs, Analytical and Environmental Chemistry Department, Vrije Universiteit Brussel, Pleinlaan 2, Brussels B-1050, Belgium.
- S. H. M. Jacquet, Centre Européen de Recherche et d'Enseignement des Géosciences de l'Environnement (CEREGE), BP 80, 13545 Aix en Provence, France. (jacquet@cerege.fr)
- N. Savoye, Observatoire Aquitain des Sciences de l'Univers, UMR 5805 EPOC, CNRS, Université Bordeaux 1, Station Marine d'Arcachon, 2 Rue du Pr. Jolyet, F-33120 Arcachon, France.
- V. H. Strass, Alfred Wegener Institute for Polar and Marine Research, Postfach 120161, Bremerhaven D-27515, Germany.